Upper Oligocene–Lower Miocene Gangdese Conglomerate Along the Yarlung-Zangbo Suture Zone and its Implications for Palaeo-Yarlung-Zangbo Initiation

Keke Ai[1]*, Kexin Zhang[2,3]*, Bowen Song[2], Tianyi Shen[4] and Junliang Ji[3]

[1]School of Resource and Environmental Engineering, Mianyang Teachers' College, Mianyang, China, [2]Institute of Geological Survey, China University of Geosciences, Wuhan, China, [3]State Key Laboratory of Biological and Environmental Geology, China University of Geosciences, Wuhan, China, [4]School of Earth Science, China University of Geosciences, Wuhan, China

The upper Oligocene–lower Miocene Gangdese conglomerate is deposited along the Yarlung-Zangbo suture zone, which extends 1,500 km from west to east and is located in the core area of the India–Eurasia plate collision zone. The Gangdese conglomerate records richly uplift and denudation histories of the Lhasa terrane and Tethyan Himalaya on both sides of the suture zone, thus revealing the growth process of the southern Tibetan Plateau during the Late Oligocene–Early Miocene. In this study, we documented the detailed sedimentology and chronology of the Gangdese conglomerate. The Gangdese conglomerate is dominated by conglomerate and sandstone, with minor volumes of siltstone and tuff deposited in an alluvial fan and fluvial system. Based on sedimentology and structural relationships, we suggest that the Gangdese conglomerate was deposited in an extensional tectonic environment in the early period and an extrusion tectonic environment in the late period, which was controlled by Indian slab shearing and breakoff during the Late Oligocene–Miocene. According to the new magnetostratigraphy and detrital zircon U-Pb dating, the main depositional age of the Gangdese conglomerate was likely the Late Oligocene–Early Miocene (26–18 Ma), and it trended younger from west to east. Moreover, paleocurrent data from the Gangdese conglomerate showed westward axial sediment transport; thus, we inferred that a westward axial palaeo-Yarlung-Zangbo River occurred along the whole Yarlung-Zangbo suture zone during the Late Oligocene–Early Miocene, and its flow was opposite to that of the current Yarlung-Zangbo River.

Keywords: sedimentology, depositional age, Gangdese conglomerate, Late Oligocene–Early Miocene, Palaeo-Yarlung-Zangbo River

1 INTRODUCTION

A narrow Cenozoic conglomerate unit is deposited in unconformity above in the north part of the Yarlung-Zangbo suture zone, which extends 1,500 km from west to east and is located in the core area of the India–Eurasia plate collision zone (Wang J.-G. et al., 2013; Zhang et al., 2013a) (**Figure 1**). Numerous local names have been given to these rocks along the strike, such as the Kailas

FIGURE 1 | General geologic map of southern Tibet, modified after Yin (2006). Study area is outlined in red. Major faults: MFT, Main Frontal Thrust; MBT, Main Boundary Thrust; MCT, Main Central Thrust; STDS, South Tibetan Detachment System; GCT, Great Counter Thrust; KKF, Karakoram Fault. Major sutures: YTSZ, Yarlung-Zangbo suture zone.
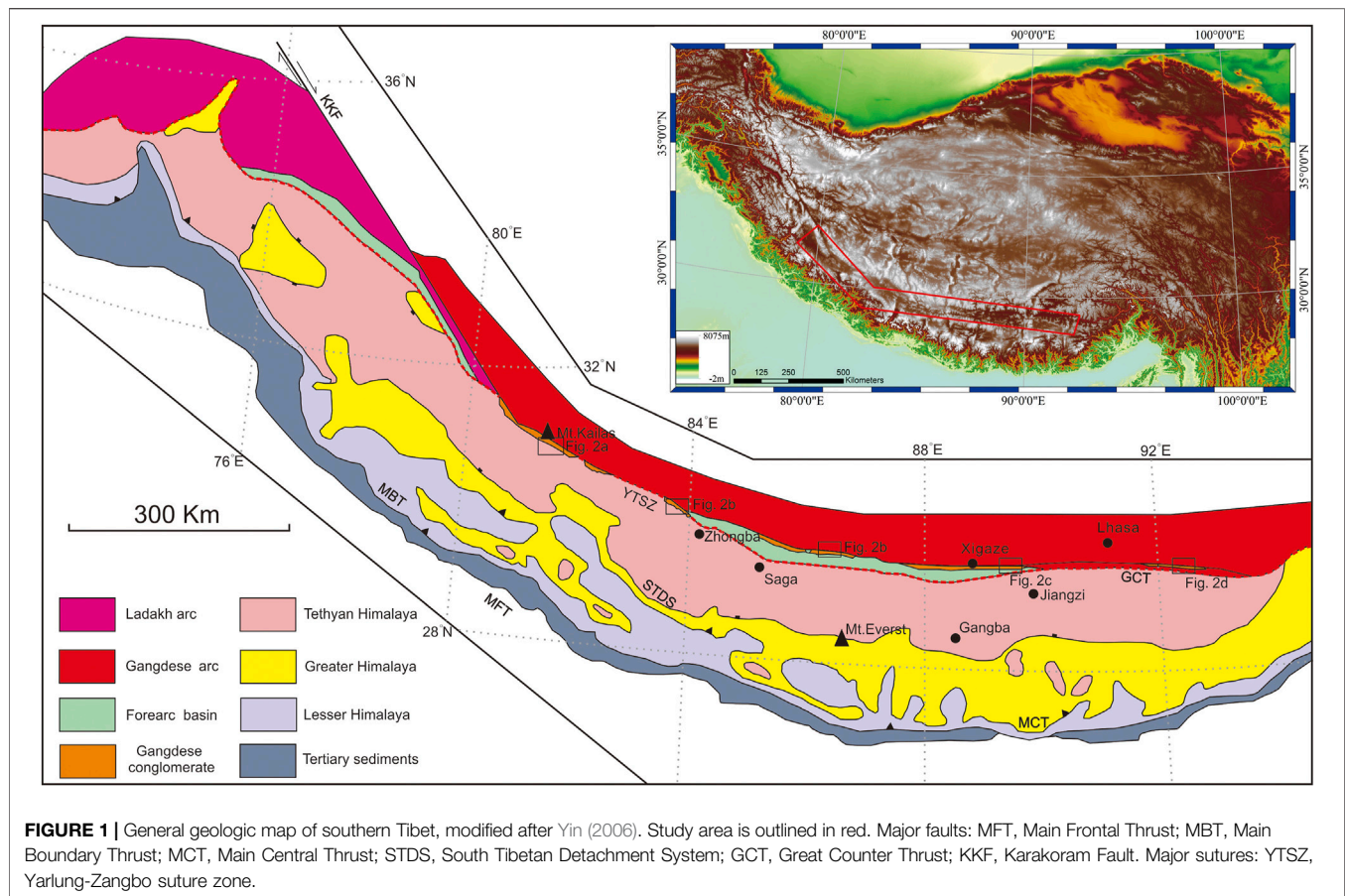
conglomerate (Gansser, 1964) and the Kailas Formation (DeCelles et al., 2011) in the western part of the suture zone and the Qiuwu (Wang J.-G. et al., 2013), Dazhuka (Aitchison et al., 2009), and Luobusa Fms. (Yin et al., 1999) in the central segment of the suture zone. Aitchison et al. (2002) grouped all of these units into the Gangrinboche Conglomerates, whereas Wang et al. (2013a) referred to this group of rocks as the Gangrinboche Conglomerate, and Li et al. (2017) referred to this group of rocks as the Gangdese Conglomerates. Therefore, in this study, we use the name "Gangdese conglomerate" to refer to the entire east–west extent of these lithologically and structurally similar sedimentary rocks.

As an important geological unit in the Yarlung-Zangbo suture zone, the Gangdese conglomerate records the detailed uplift and denudation histories of the Lhasa terrane and Tethyan Himalaya on both sides of the suture zone and reveals the growth process of the southern Tibetan Plateau during the Late Oligocene–Early Miocene (Aitchison et al., 2002; DeCelles et al., 2011; Wang J.-G. et al., 2013; Carrapa et al., 2014; DeCelles et al., 2016; Leary et al., 2016; Li et al., 2017). Hence, timing the evolution of the Gangdese conglomerate remains a fundamental problem in understanding the post-collisional tectonics of southern Tibet. In the early stage, palaeontological fossils and stratigraphic correlations were used to define the sedimentary age of the Gangdese conglomerate. Due to the lack of index fossils and marker layers, the ages obtained

with these methods ranged from Jurassic to Early Miocene (Guo, 1975; Geng and Tao, 1982; Li, 2004; Li et al., 2009; Li et al., 2010). Recently, U-Pb zircon dating of volcanic interlayers and detrital zircon dating of sandstone in the Gangdese conglomerate have suggested that the sedimentary age of the Gangdese conglomerate is Late Oligocene to Early Miocene (Aitchison et al., 2002; DeCelles et al., 2011; Wang J.-G. et al., 2013; Carrapa et al., 2014; DeCelles et al., 2016; Leary et al., 2016). Li et al. (2017) proposed that the Gangdese conglomerate extended from Late Oligocene to Late Miocene.

Based on the constrained age of the Gangdese conglomerate, various tectonic models have been proposed. For instance, Aitchison et al. (2002, 2007) proposed that the India–Asia collision did not occur until the mid-Cenozoic (ca. 34 Ma) based partly on the interpretation of the Gangdese conglomerate, and this result differs greatly from the currently prevailing views of ca. 65–50 Ma (e.g., Garzanti et al., 1987; Ding et al., 2005). DeCelles et al. (2011), DeCelles et al. (2016) and Wang et al. (2013a) studied the Gangdese conglomerate in the Kailas Basin and Qiabulin area of Xigaze and pointed out that the lower strata of the Gangdese conglomerate were formed under an extensional tectonic setting, whereas the upper strata were formed under a compression background, thus representing the reversal and detachment of the subducted Indian plate during the Oligocene to Early Miocene. Li et al. (2017)
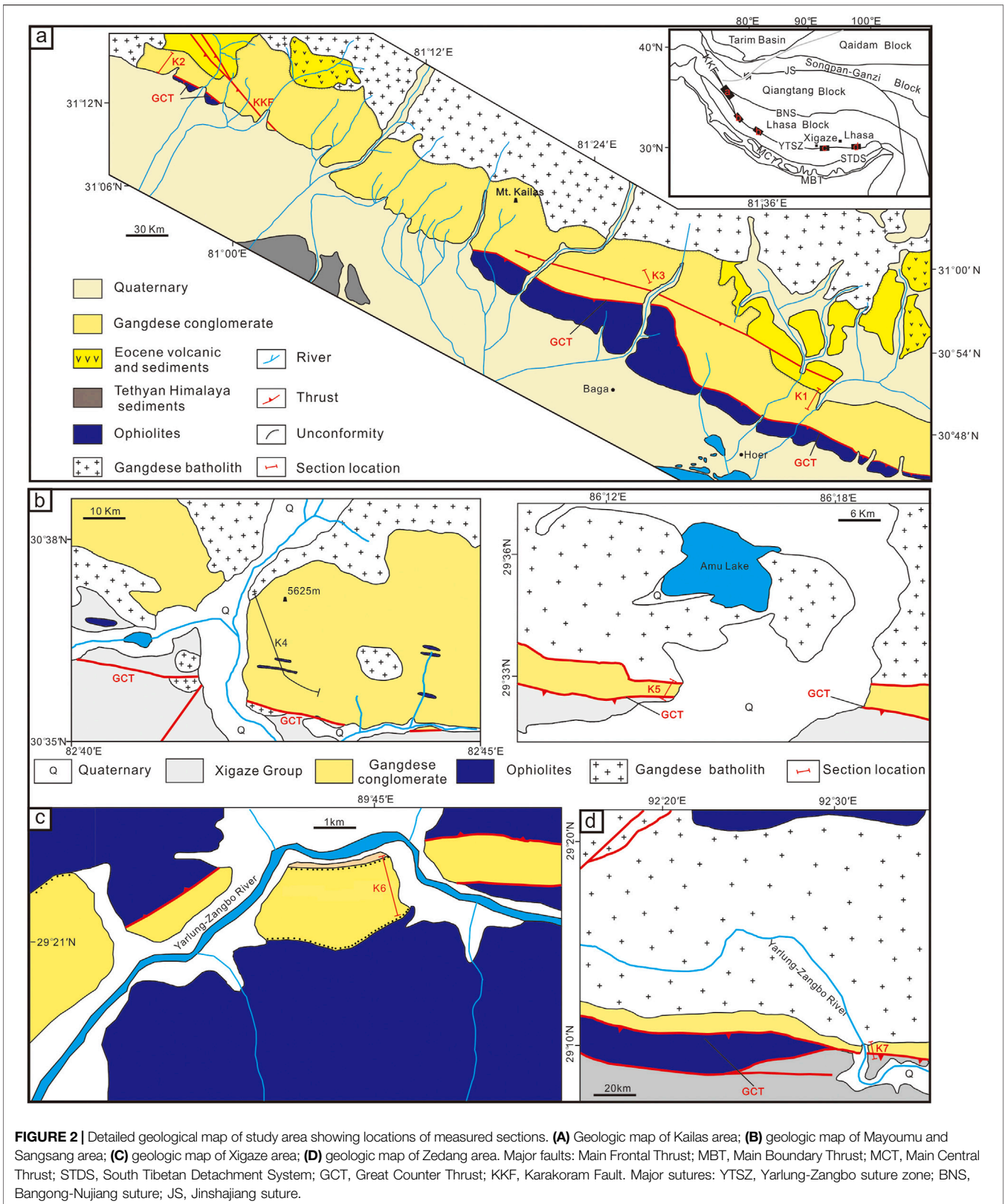
FIGURE 2 | Detailed geological map of study area showing locations of measured sections. **(A)** Geologic map of Kailas area; **(B)** geologic map of Mayoumu and Sangsang area; **(C)** geologic map of Xigaze area; **(D)** geologic map of Zedang area. Major faults: Main Frontal Thrust; MBT, Main Boundary Thrust; MCT, Main Central Thrust; STDS, South Tibetan Detachment System; GCT, Great Counter Thrust; KKF, Karakoram Fault. Major sutures: YTSZ, Yarlung-Zangbo suture zone; BNS, Bangong-Nujiang suture; JS, Jinshajiang suture.

performed a comprehensive study of the Gangdese conglomerate in southern Tibet and suggested that it was formed in different tectonic settings at different locations. In the Kailas Basin, the deposition of the Gangdese conglomerate was closely related to the Karakoram Fault (KKF) and Great Counter Thrust (GCT), which were mainly formed under extensional or torsional environments. However, in the Xigaze and Zedang areas, the deposition of the Gangdese conglomerate was associated with the development of the Gangdese Thrust (GT) and GCT in a compressional tectonic regime (Yin et al., 1994; Yin et al., 1999). Leary et al. (2016) studied the Gangdese conglomerate in Lazi and Xigaze and argued that the deposition of the Gangdese conglomerate was controlled by Indian slab shearing and breakoff during the Late Oligocene–Early Miocene, which began in western Tibet around 26 Ma and reached eastern Tibet by ca. 18 Ma. Using the new thermochronological data and modeling of samples from the Gangdese batholith in southwestern Tibet, et al. (2020) illustrated that not only the Kailas Basin but also over a relatively large region in southern Tibet were topographically depressed. After being exposed at the surface, the Gangdese batholith experienced reheating during burial beneath the Kailas Formation between ~28–26 and 21–20 Ma, followed by rapid cooling between 20 and 17 Ma. Previous chronology and structural relationship studies indicate that the main depositional age of the Gangdese conglomerate was likely the Late Oligocene–Early Miocene (26–18 Ma), and it trended younger from west to east. However, the Gangdese conglomerate age, mainly controlled by detrital zircons and tuff layer, requires more dating data from different methods and outcrops to accurate the east youth trend.

The Gangdese conglomerate is preserved along the present-day course of the Yarlung-Zangbo River and more likely records the sedimentation of the palaeo-Yarlung-Zangbo fluvial system (Wang L. et al., 2013; Li et al., 2017). Previous palaeocurrent data from the Gangdese conglomerate indicate a west to northwestward sediment transport, implying that the palaeo-Yarlung-Zangbo River once flowed westward (Wang L. et al., 2013; Li et al., 2017). However, previous studies have only indicated that the palaeo-Yarlung-Zangbo River once flowed westward in the studied areas, but if there was a westward axial palaeo-Yarlung-Zangbo River that occurred along the whole Yarlung-Zangbo suture zone still remain to be investigated. Hence, new palaeocurrent measurement and age and provenance data from the Gangdese conglomerate are presented here to illustrate the evolution of the Yarlung-Zangbo River.

Although abundant research results have been obtained, many problems remain to be solved, including the exact east youth trend age constraint for the Gangdese conglomerate and reconstruction of the palaeo-Yarlung-Zangbo fluvial system. In this paper, we measured seven sections of the Late Oligocene–Early Miocene Gangdese conglomerate (K1–K7) along the Yarlung-Zangbo River valley (**Figures 1**, **2**) and established a new chronostratigraphy framework for the Gangdese conglomerate. Based on the new age control, we thus studied the sedimentology and provenance of the seven Gangdese conglomerate sections, produced a sedimentary-tectonic model of the Gangdese conglomerate, and further

discussed the implications of these findings for the evolution of the Yarlung-Zangbo River.

2 STRATIGRAPHY AND SEDIMENTOLOGY

The E–W distributed Gangdese conglomerate crops out along the southern flank of the Gangdese arc, north of the Yarlung-Zangbo suture zone (**Figure 1**). Based on the detailed study of the lithofacies and lithofacies assemblages and combined with the sedimentary structure, we identified a total of 10 types of lithofacies in the section of the Gangdese conglomerate and divided the Gangdese conglomerate into four facies: braided river, alluvial fan, fan delta, and lacustrine facies (**Figure 3**). The observed lithofacies and process interpretations are listed in **Table 1**.

2.1 Section Location

The Gangdese conglomerate sections investigated in this study are exposed along the Yarlung-Zangbo suture zone (**Figures 1**, **2**). We measured seven sections of the Late Oligocene–Early Miocene Gangdese conglomerate (K1–K7) at five well-exposed locations along the Yarlung-Zangbo River valley (**Figure 2**), and they included Kailas Basin sections (K1–K3) (**Figure 2A**), Mayoumu and Sangsang sections (K4 and K5) (**Figure 2B**), Xigaze section (K6) (**Figure 2C**), and Jiaca section (K7) (**Figure 2D**).
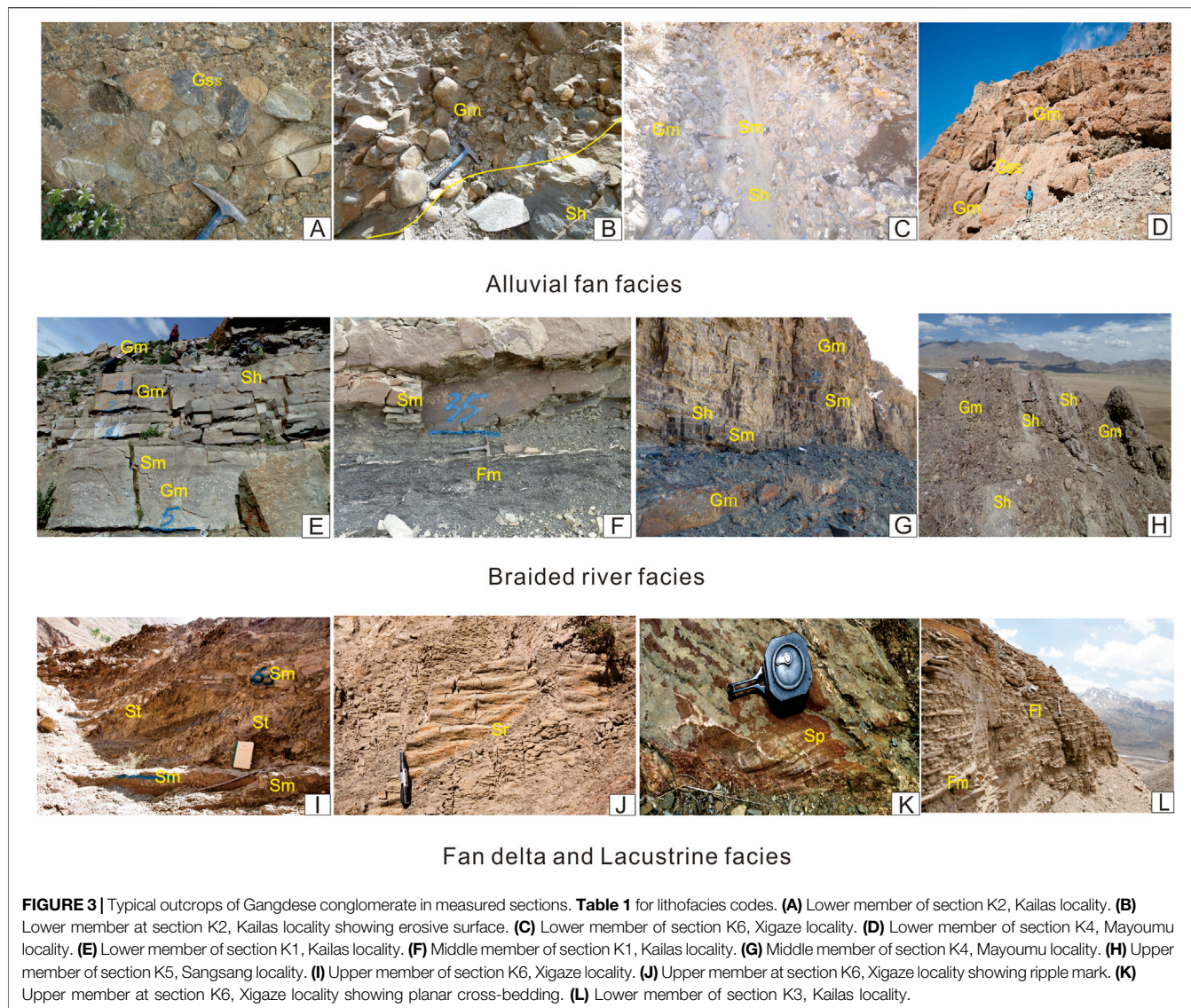
In the Kailas area, the Gangdese conglomerate is distributed NW–SE along the south side of the Gangdese bedrock. The northern side unconformably overlies the Eocene Qiuwu and Dianzhong volcanic rocks, and the southern side is separated from the Tethyan Himalaya sedimentary system and melanges by the GCT. We measured three well-exposed sections of the Gangdese conglomerate, numbered K1, K2, and K3 (**Figures 1 and 2A**).

In the Mayoumu area, the Gangdese conglomerate unconformably overlies Gangdese bedrock and is covered by Quaternary rocks of ~500-m thickness (**Figures 1**, **2B**). In the Sangsang area, the Gangdese conglomerate is in fault contact with the underlying Gangdese bedrock and overlying Xigaze Group. (**Figures 1**, **2B**). In the Xigaze and Jiaca area, the Gangdese conglomerate is in fault contact with the Gangdese bedrock, Xigaze Group, and ophiolite (**Figures 1**, **2C**, **D**).

2.2 Facies and Interpretation
2.2.1 Alluvial Fan Facies
Alluvial fan facies are mainly distributed in the bottom part of K2, the upper part of K3, the bottom and upper parts of K4, K5, and K6, and in K7 (**Figures 3**, **4**), and they are composed of Gm, GSs, Sh, Sp, and Fl. Gm is mainly composed of poor sorting and matrix-supported gravels, which are subangular to subrounded and mostly 5–15 cm in diameter. The gravel content of the conglomerate is approximately 40–60%, and the main ingredients are quartzite, andesite, silicalite, and tuff. The single Gm is generally approximately 1–2-m thick and often presents an imbrication structure (Gm) or grain sequence (GSs).

FIGURE 3 | Typical outcrops of Gangdese conglomerate in measured sections. **Table 1** for lithofacies codes. **(A)** Lower member of section K2, Kailas locality. **(B)** Lower member at section K2, Kailas locality showing erosive surface. **(C)** Lower member of section K6, Xigaze locality. **(D)** Lower member of section K4, Mayoumu locality. **(E)** Lower member of section K1, Kailas locality. **(F)** Middle member of section K1, Kailas locality. **(G)** Middle member of section K4, Mayoumu locality. **(H)** Upper member of section K5, Sangsang locality. **(I)** Upper member of section K6, Xigaze locality. **(J)** Upper member at section K6, Xigaze locality showing ripple mark. **(K)** Upper member at section K6, Xigaze locality showing planar cross-bedding. **(L)** Lower member of section K3, Kailas locality.

The parallel bedding (Sh and Sm), planar cross-bedding (Sp), and erosive base in the pebbled coarse sandstone and coarse sandstone represent the alluvial fan foot to middle deposits. Fl is a magenta medium-fine conglomerate with thin-bedded sandstone and siltstone that represents alluvial fan distal deposits.

2.2.2 Braided River Facies

Braided river facies are commonly distributed in the middle part of the Gangdese conglomerate (K1–K6) (**Figures 3**, **4**), and they are composed of Gm, GSs, Sh, Sp, Sm, and Fm. Gm is variegated, gray, white, and magenta medium-thick conglomerate intercalated with medium-thin sandstone. The conglomerate is clast supported, poorly sorted, and subangular to subrounded. The main particle size is 5–10 cm, and the large particles are around 20 cm. Imbricate structures and intercalated sandstone are partly in the conglomerate. Parallel bedding and planar cross-bedding are widely distributed in pebbled coarse sandstone and coarse sandstone, and bedded terrane sandstone represents

channel sand bar depositions. There are multiple sequences of conglomerate–sandstone–siltstone–mudstone, which represent multiple flooding events. The Fm is gray to grayish-black thin-layer fine sandstone, siltstone, and mudstone, representing braided river floodplain deposition.

2.2.3 Fan Delta Facies

Fan delta facies are mainly distributed in the middle to the upper part of K3 and the upper part of K6 (**Figures 3**, **4**), and they are composed of Gc, Gm, GSs, Sp, Sh, St, and Sm. Gc is a magenta medium-thick coarse conglomerate with some boulders. The gravel is clast supported, the main particle size of the gravel is 3–5 cm, and the larger gravel can reach 10 cm. In some areas, the gravel may be imbricated or interbedded with yellowish medium-coarse sandstone. Sp, Sh, and Sm are gray-yellow thick-layer coarse sandstones and pebbly coarse sandstones with parallel bedding and planar cross-bedding, and some sandstones are thick and massive.

TABLE 1 | Lithofacies used in measured sections and interpretations in this study.

Lithofacies code	Description	Interpretation
Gm	Massive, matrix-supported pebble-cobble conglomerate, poorly sorted, disorganized, unstratified	Deposition by cohesive mud-matrix debris flows
Gss	Poorly sorted, thin layer or lenticular, heterogeneous-particle support, coarse sand to coarse grain	Gravity flow deposition
Gc	Massive, clast-supported, granule-pebble conglomerate	Debris flows
Sh	Fine- to medium-grained sandstone with plane-parallel lamination	Upper plane bed conditions under unidirectional flows, either strong (>100 cm/s) or very shallow
Sm	Massive medium- to fine-grained sandstone	Sandy mudflows and suspension settling in lake and overbank deposits
St	Medium- to very coarse-grained sandstone with trough cross-stratification	Migration of large 3D ripples (dunes) under moderately powerful (40–100 cm/s) unidirectional flows in channels
Sp	Medium- to very coarse-grained sandstone with planar cross-stratification	Migration of large 2D ripples under moderately powerful (40–60 cm/s) unidirectional channelized flows: migration of sandy transverse bars
Sr	Fine- to medium-grained sandstone with small, asymmetric 2D and 3D current ripples	Migration of small 2D and 3D ripples under weak (20–40 cm/s) unidirectional flows in shallow channels
Fl	Laminated very fine-grained sandstone, siltstone, or mudstone	Distal fan, floodplain. abandoned channel deposits or suspension-setting
Fm	Massive mudstone to fine-grained sandstone with common gray mottling and gypsum veins	Suspension settling in lake and overbank deposits

Note: Modified after (Miall, 1984, 1996).
2D, two-dimensional; 3D, three-dimensional

2.2.4 Lacustrine Facies

The lacustrine facies are mainly distributed in the bottom part of K3 and upper part of K6 (**Figures 3, 4**), and they are composed of Sp, Sh, Sr, Fm, and Fl. Sp is gray medium-coarse sandstone, yellow thick-layer sandstone intercalated with a conglomerate lens with planar cross-bedding. Sh is gray and yellowish fine sandstone with a ripple mark (Sr). Fm is grayish-black thin-layer muddy siltstone and bluish thin layer fine sandstone with horizontal bedding. Fl is bluish-gray thin siltstone and thin muddy siltstone, yellowish fine sandstone and siltstone, and grayish-yellow fine sandstone.

Based on detailed field outcrop observations and sedimentary facies analyses combined with the results of previous studies, the Gangdese conglomerate is mainly composed of conglomerate and sandstone, with minor volumes of siltstone and tuff. The Gangdese conglomerate consists of multiple sedimentary cycles, with each cycle presenting a suite of fining-upward sequences.

3 DEPOSITIONAL AGE CONSTRAINTS

The age of the Gangdese conglomerate has been determined based on U-Pb zircon ages from tuff samples, the youngest populations of detrital zircon ages, and the magnetostratigraphy.

3.1 Zircon U-Pb Dating Method

In this study, nine sandstone samples were collected for zircon U-Pb dating, and the sample locations are shown in **Figure 4**. The age was determined by measuring the U-Pb ages of zircon using the multi-collector laser ablation inductively coupled plasma mass spectrometry (MC-LA-ICP-MS) system at the State Key Laboratory of Geological Processes and Mineral Resources (GPMR), China University of Geosciences, Wuhan. Detrital zircon samples U-Pb data shown in **Supplementary**.

In the Kailas area, three detrital zircon samples (K1–30D, K2–10D, and K3–35D) show that the youngest detrital zircon U-Pb ages are 23–26 Ma (**Figure 5**), thus constraining the maximum depositional age of this stratigraphic level to the Late Oligocene to Early Miocene.

In the Mayoumu and Sangsang areas, two detrital zircon samples (K4–36D and K5–5D) show that the youngest detrital zircon U-Pb ages are 42–23.6 Ma (**Figure 5**), with five around the 23.6 Ma, thus constraining the maximum depositional age of this stratigraphic level to the Late Oligocene.
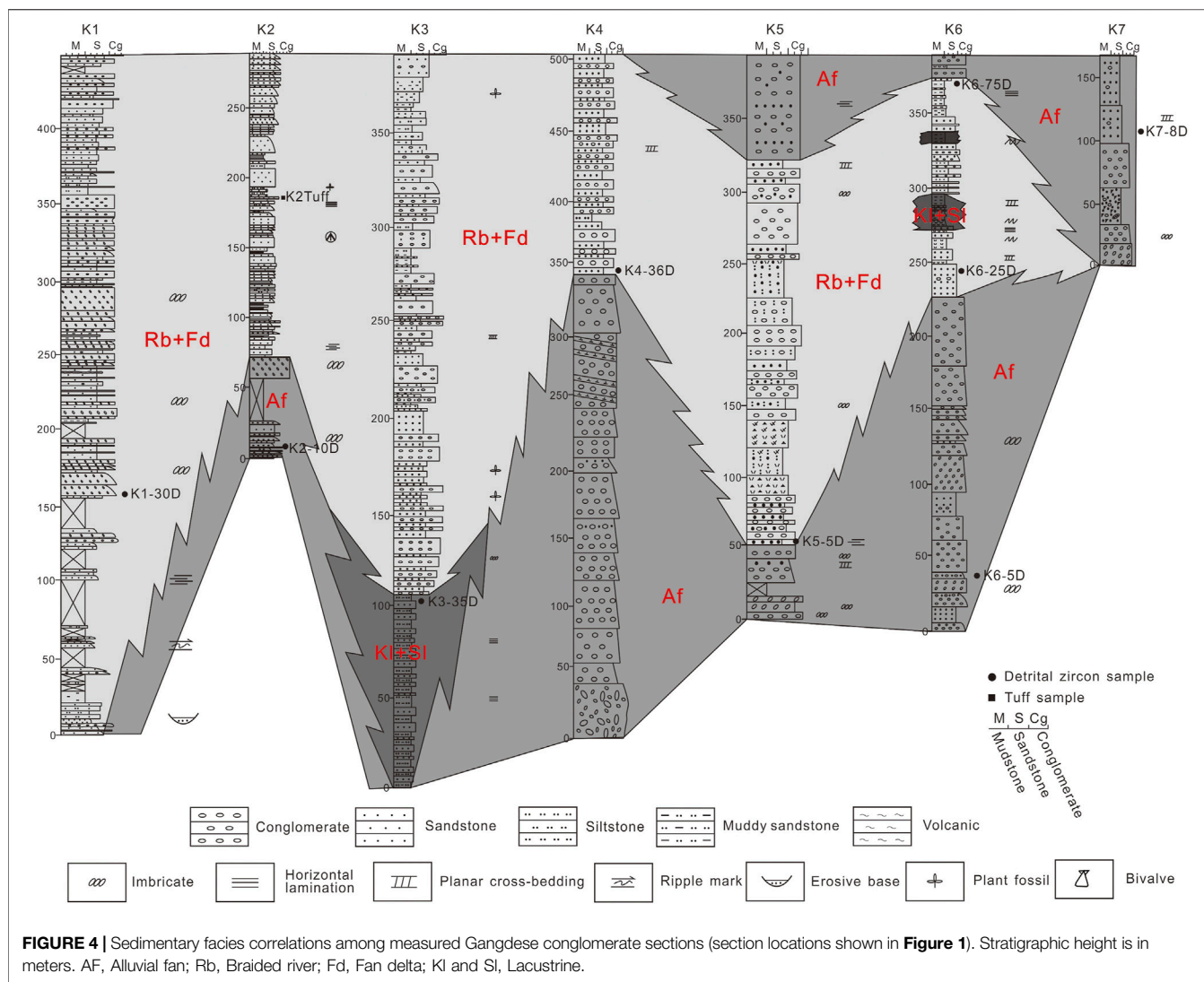
In the Xigaze area, three detrital zircon samples (K6–5D, K6–25D, and K6–75D) show that the youngest detrital zircon U-Pb ages are 20.3–24 Ma (**Figure 5**), thus constraining the maximum depositional age of this stratigraphic level to the Late Oligocene to Early Miocene.

In the Jiacha area, although one detrital zircon sample was used for U-Pb dating (K7–8D), the youngest detrital zircon U-Pb ages are around 100–200 Ma, so we did not obtain the age constraint for the Gangdese conglomerate. However, previous studies showed that the Gangdese conglomerate was deposited during the Late Oligocene to Early Miocene in the Jiacha area (Aitchison et al., 2009; Li et al., 2017).

3.2 Magnetostratigraphy

A total of 170 oriented palaeomagnetic samples were collected in the K2 section of the Gangdese conglomerate to obtain high-resolution magnetostratigraphy. The ChRM directions obtained from the K2 section were used to calculate the virtual geomagnetic pole (VGP) latitudes and define the geomagnetic polarity zones, and they showed that the K2 section containing the plant fossil layer spans an age range of 25.1–21.8 Ma (Ai et al., 2019).

Based on the discussion earlier and previous studies (Aitchison et al., 2002; DeCelles et al., 2011; Wang L. et al., 2013; Carrapa et al., 2014; DeCelles et al., 2016; Leary et al., 2016; Li et al., 2017), the depositional age of the Gangdese conglomerate in the Kailas area

FIGURE 4 | Sedimentary facies correlations among measured Gangdese conglomerate sections (section locations shown in **Figure 1**). Stratigraphic height is in meters. AF, Alluvial fan; Rb, Braided river; Fd, Fan delta; Kl and Sl, Lacustrine.

(81–83°E) was mainly 22–26 Ma (**Figures 5**, **6**), at 23–25 Ma in Sangsng and Lazi (85–88°E) (**Figures 5**, **6**), at 19–23 Ma near Xigaze and Dazhuka (89–90°E) (**Figures 5**, **6**), and as late as 17–18 Ma in Zengdang (91–92°E) (**Figures 5**, **6**). However, Li et al. (2017) exhibited the youngest age cluster of 4.3–6.1 Ma ($n = 9$) from one sample in the Kailas area, constraining the maximum depositional age of this stratigraphic level to the Late Miocene to Early Pliocene in the Kailas area. This young age is very different from our study and previous data. Combined with our study and many other data in the Kailas area, we inferred that the depositional age of the Gangdese conglomerate in the Kailas area was mainly 22–26 Ma. Overall, we suggested that the main depositional age of the Gangdese conglomerate was likely the Late Oligocene–Early Miocene, and it trended younger from west to east (**Figures 5**, **6**).

4 PROVENANCE AND PALAEOCURRENT

Integrated palaeocurrent, petrologic, and geochronological approaches were implemented to analyze the provenance of the Gangdese conglomerate.

4.1 Palaeocurrent Data
Unidirectional palaeocurrent orientations were primarily measured from imbricated clasts, planar cross-bedding, and flute casts preserved within sandstone and conglomerate beds. The measurements were corrected with horizontal bedding rotations.

In the Kailas area, the palaeocurrent data from the bottom part of the K1 and K2 sections indicate mainly southward palaeoflow
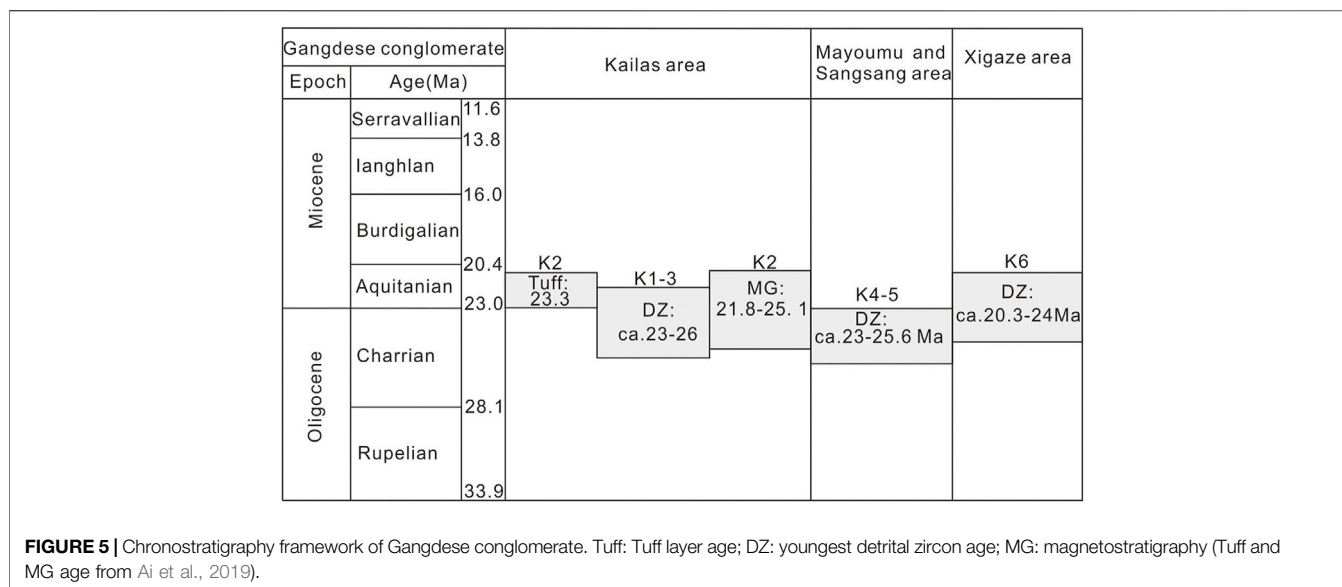
FIGURE 5 | Chronostratigraphy framework of Gangdese conglomerate. Tuff: Tuff layer age; DZ: youngest detrital zircon age; MG: magnetostratigraphy (Tuff and MG age from Ai et al., 2019).
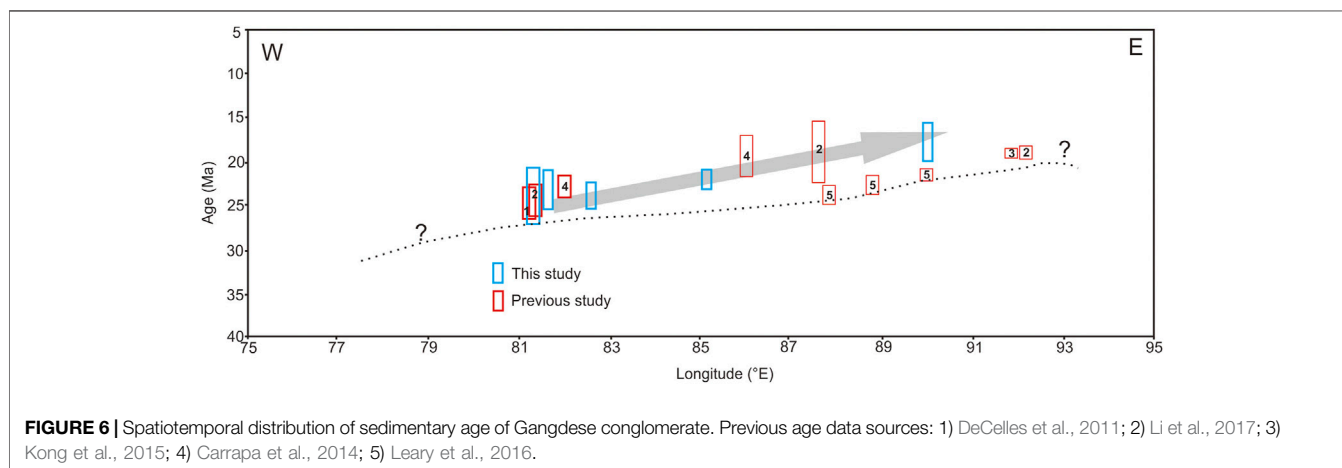
FIGURE 6 | Spatiotemporal distribution of sedimentary age of Gangdese conglomerate. Previous age data sources: 1) DeCelles et al., 2011; 2) Li et al., 2017; 3) Kong et al., 2015; 4) Carrapa et al., 2014; 5) Leary et al., 2016.

directions, suggesting a northern source. In contrast, in the upper part of the K2 section and K3 section, the palaeocurrent data measured from imbricated clasts and cross-bedding record not only southward but also northward palaeoflow directions, indicating that sediments were derived from both sides of the Yarlung-Zangbo suture zone (**Figure 7**).
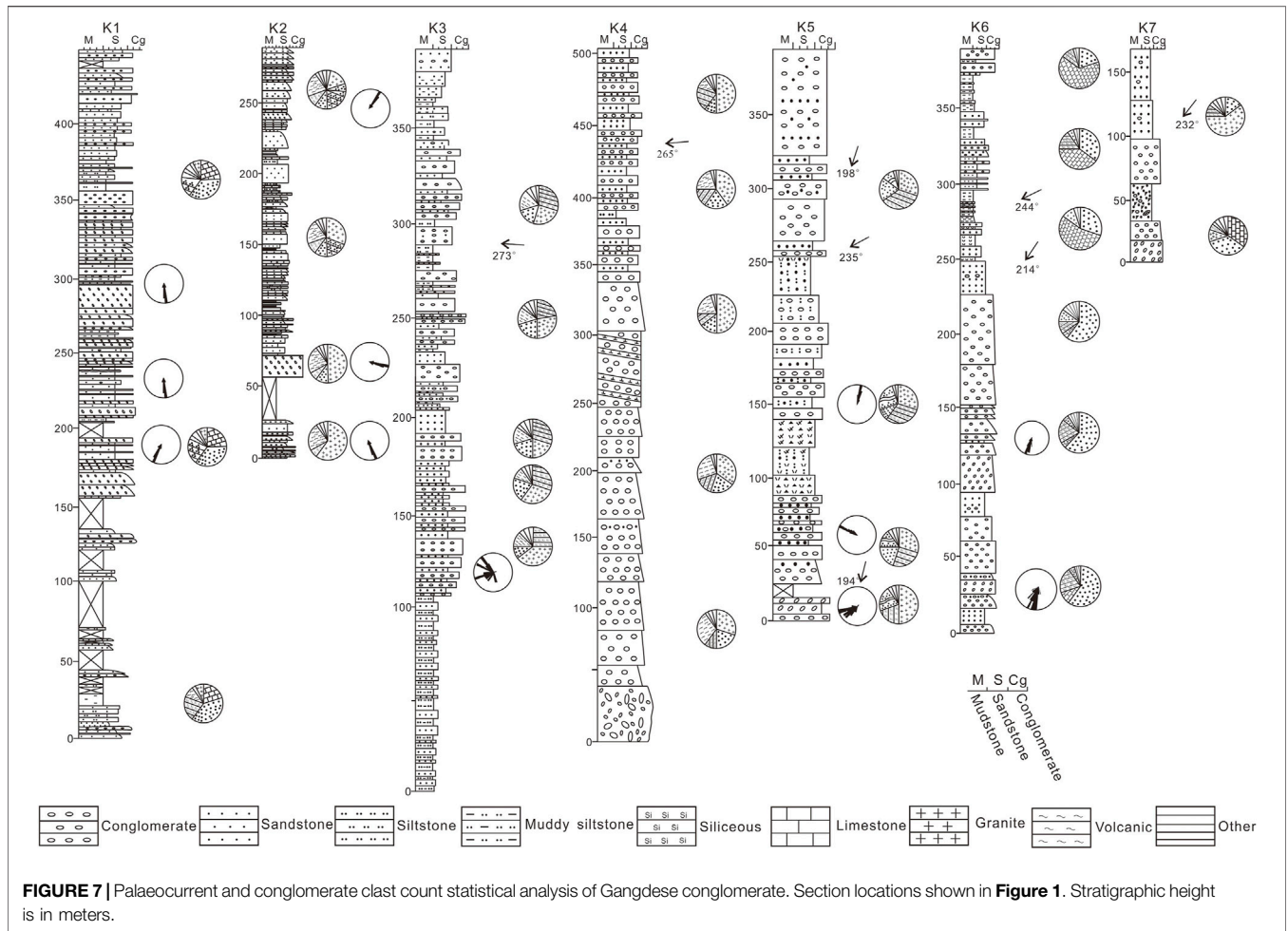
In the Mayoumu and Sangsang areas, the palaeocurrent data measured from cross-bedding in the K4 section record a westward palaeoflow direction, and the palaeocurrent data measured from the K5 section record mainly a northwestward palaeoflow direction and a southeast palaeoflow direction (**Figure 7**).

In the Xigaze area, the palaeocurrent data measured from imbricated clasts and cross-bedding in the lower part of the K6 section record a southwestward palaeoflow direction and change to a northwestward palaeoflow direction in the upper part of the K6 section. In the Jiacha area, the palaeocurrent data measured

from the K7 section record mainly southwestward palaeoflow directions (**Figure 7**).

4.2 Conglomerate Clast Counts

At least 100 clasts were counted at each station. In the Kailas area, the conglomerates of the lower part of the Gangdese conglomerate (the bottom of K1 and K2) are dominated by granite, volcanic rock, diorite, and a small amount of siliceous rock, limestone, and sandstone (**Figure 7**), which are consistent with the lithological characteristics of the Gangdese magmatic arc. Combined with the palaeoflow directions, these results indicate that the source area should be the Gangdese magmatic arc in the north. In contrast, in the upper part of Gangdese conglomerate (upper part of K2 and K3), the conglomerates are dominated by not only granite, volcanic rock, and diorite but also large amounts of sandstone

FIGURE 7 | Palaeocurrent and conglomerate clast count statistical analysis of Gangdese conglomerate. Section locations shown in **Figure 1**. Stratigraphic height is in meters.

and siltstone, siliceous rocks, and limestones from the southern Tethyan Himalaya, indicating that the sediments were derived from both sides of the Yarlung-Zangbo suture zone (**Figure 7**).

In the Mayoumu area, the conglomerates of the K4 section are dominated by granite and volcanic rocks and have a small amount of sandstone and siliceous rocks. There is no significant vertical change in the gravel composition, although the granite gravel content is significantly reduced upward (**Figure 7**). In the Sangsang area, the conglomerates of the K5 section are dominated by granite, siliceous rock, quartzite, and sandstone, and the contents of quartz sandstone and quartzite increase upward (**Figure 7**). Granite and sandstone gravel are mainly from the Gangdese magmatic arc and Lhasa terrane on the north side, quartzite and quartz sandstone are from the Tethyan Himalaya on the south side, and clasts from the south side show an increasing trend.

In the Xigaze area, the conglomerates of the lower part of the K6 section are dominated by granite, siliceous rock, and sandstone. In contra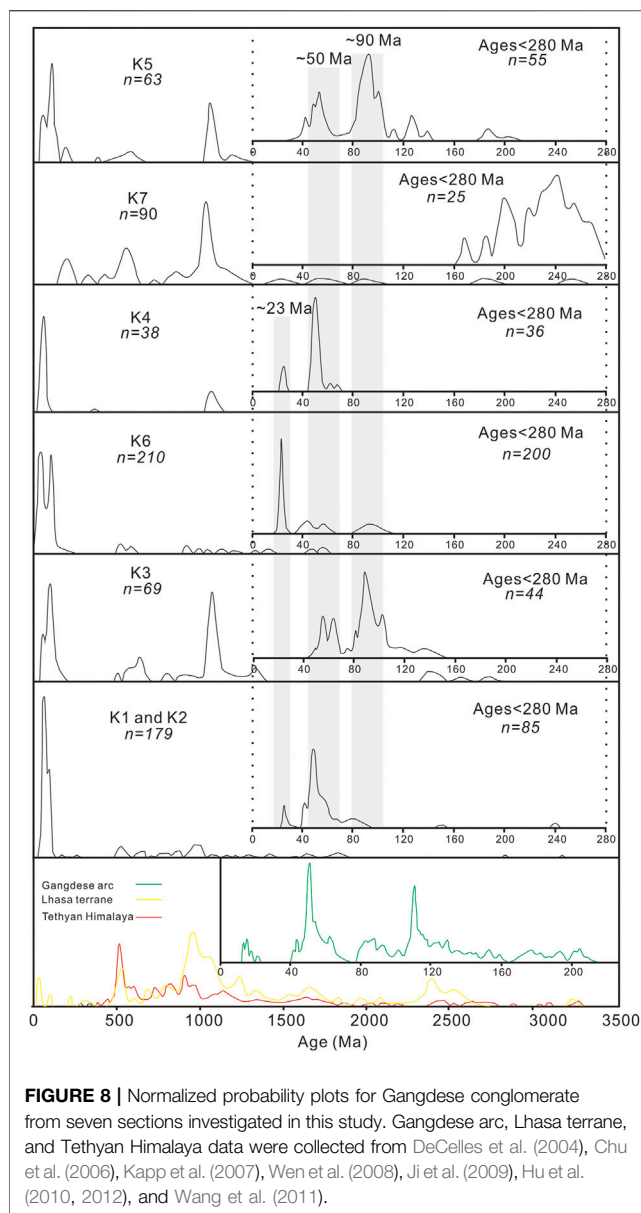st, the upper part of the K6 section is dominated by limestone and bits of basic and ultrabasic gravel (**Figure 7**). Granite gravels are mainly from the Gangdese in the north, and sandstone and limestone gravels from the Lhasa terrane in the north or the Xigaze forearc basin in the south, whereas basic and ultrabasic gravels are from the ophiolite melange in the Yarlung-Zangbo suture zone in the south.

In the Jiacha area, the conglomerates of the K7 section are dominated by granite, limestone, and siliceous rock (**Figure 7**), and the sediments are derived from both sides of the Yarlung-Zangbo suture zone.

Based on the detailed statistical analysis of gravel composition discussed earlier and combined with the palaeocurrent data, the provenance of the lower part of the Gangdese conglomerate was mainly the Gangdese arc and Lhasa terrane, whereas that of the upper part of the Gangdese conglomerate included both sides of the Yarlung-Zangbo suture zone.

4.3 U-Pb Detrital Ages

In the Kailas area, two sandstone samples were collected from the K1 and K2 sections (K1–30D and K2–10D) for detrital zircon

FIGURE 8 | Normalized probability plots for Gangdese conglomerate from seven sections investigated in this study. Gangdese arc, Lhasa terrane, and Tethyan Himalaya data were collected from DeCelles et al. (2004), Chu et al. (2006), Kapp et al. (2007), Wen et al. (2008), Ji et al. (2009), Hu et al. (2010, 2012), and Wang et al. (2011).

U-Pb dating, and 179 usable ages were obtained (**Figure 8**). The zircon crystals were mostly euhedral, and high Th/U ratios (>0.1) were observed in 98% of the total grains, which is suggestive of an igneous origin (Belousova et al., 2002). The age spectra are dominated by ages younger than 280 Ma, with main age peaks at 23 and 50 Ma, which is identical to the age pattern of the Gangdese arc (e.g., Ji et al., 2009). A small number of ages distributed from 160–260 Ma were consistent with the age of the red layer in the Lhasa terrane (Carrapa et al., 2014). The age distributions greater than 280 Ma were loose and mainly contained 500, 1,000, and 1,500 Ma, and they may have been

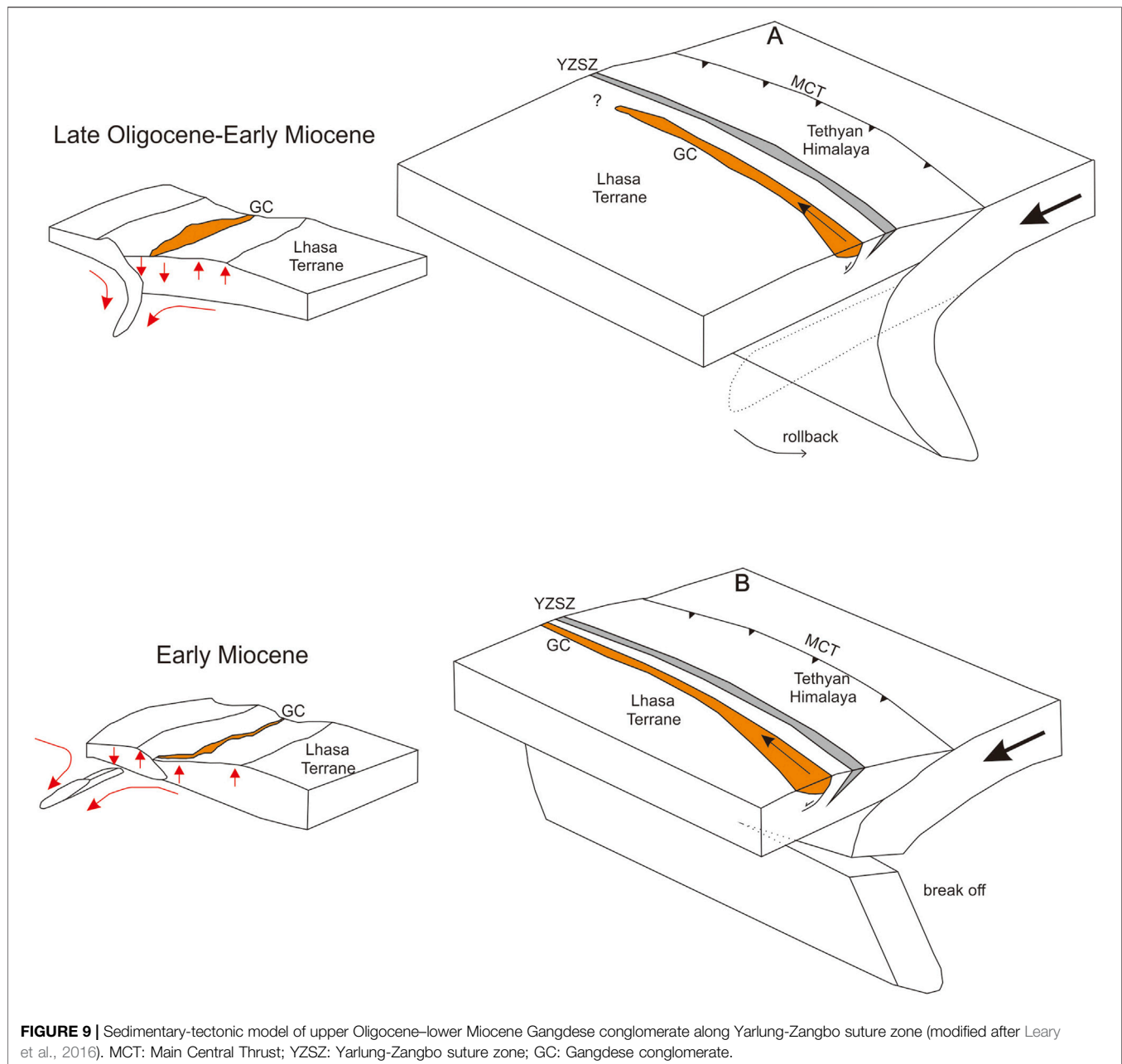associated with the Lhasa terrane in the north and the Tethyan Himalaya in the south (**Figure 8**).

One sandstone sample was collected from the K3 section (K3–35D) for detrital zircon U-Pb dating, and 69 usable ages were obtained (**Figure 8**). The zircon crystals were mostly euhedral, and no more than 1% of the zircon Th/U ratios had values <0.1. The age spectra were mainly distributed between 40 and 160 Ma, with main age peaks at 50 and 90 Ma, which is identical to the age pattern of the Gangdese arc in the north, and the significant peak age at 1,062 Ma is from the Lhasa terrane (Zhu et al., 2011).

In the Mayoumu and Sangsang areas, two sandstone samples were collected from the K4 and K5 sections (K4–36D and K5–5D) for detrital zircon U-Pb dating, and 101 usable ages were obtained (**Figure 8**). The zircon crystals were mostly euhedral and had high Th/U ratios (>0.1). The age spectra of the two samples were similar and dominated by ages younger than 280 Ma (89%), with main age peaks at 23, 53, and 94 Ma, which is identical to the age pattern of the Gangdese arc in the north, and the significant peak age at 1,062 Ma was from the Lhasa terrane (Zhu et al., 2011).

In the Xigaze area, three sandstone samples were collected from the K6 section (K6–5D, K6–25D, and K6–75D) for detrital zircon U-Pb dating, and 210 usable ages were obtained (**Figure 7**). The age spectra of the three samples were similar and mainly divided into two parts: <100 and >100 Ma. The age value < 100 Ma accounts for 90%. Samples K6–5D and K6–25D from the lower part of the K6 section showed a major early Miocene (~23 Ma) peak, which was identical to the age pattern of the Gangdese arc. Combined with the palaeocurrent data of Section K6, we infer that the provenance of the lower part of K6 was mainly from the Gangdese arc in the north. The age of sample K6–75D in the upper part of the K6 section changed significantly. There were two significant age peaks at 40–60 and 80–110 Ma, which were identical to the age pattern of the Gangdese arc (Chu et al., 2006; Wen et al., 2008; Ji et al., 2009), whereas the age records of the older zircons at 500, 800–1,000, and 1,600 Ma were obtained from the Lhasa terrane in the north, the Tethyan Himalaya in the south, and the Xigaze forearc basin in the south (Hu et al., 2010; Wang et al., 2011; Hu et al., 2012) (**Figure 8**).

In the Jiacha area, one sandstone sample was collected from the K7 section (K7–8D) for detrital zircon U-Pb dating, and 90 usable ages were obtained (**Figure 8**). The age spectra were mainly distributed from 160–300 and at 1,100 Ma, which were mainly from the Lhasa terrane, whereas the age at 450–650 Ma was from the Tethyan Himalaya. Combined with the palaeoflow data, the ages between 1,400 and 3,300 Ma should be from both sides of the Yarlung-Zangbo suture zone.

Overall, according to the statistical analysis of the gravel composition and detrital zircon age spectrum, the provenance of the Gangdese conglomerate in the lower part mainly came from the Gangdese arc and Lhasa terrane, whereas that in the upper part of the Gangdese conglomerate was from both sides of the Yarlung-Zangbo suture zone. Based on the provenance analysis, we inferred that the Gangdese in the north was the main erosion source area during the early deposition of the

FIGURE 9 | Sedimentary-tectonic model of upper Oligocene–lower Miocene Gangdese conglomerate along Yarlung-Zangbo suture zone (modified after Leary et al., 2016). MCT: Main Central Thrust; YZSZ: Yarlung-Zangbo suture zone; GC: Gangdese conglomerate.

Gangdese conglomerate, and the Himalayas were at a low elevation at that time. Later, the Himalayas in the south were uplifted, becoming the main erosion source area.

5 DISCUSSION

5.1 Sedimentary-Tectonic Model of the Upper Oligocene-Lower Miocene Gangdese Conglomerate

Based on the study of chronology, sedimentology, and structural relationships, and combined with previous studies, we established

the sedimentary-tectonic model of the upper Oligocene–lower Miocene Gangdese conglomerate.

1) Late Oligocene–Early Miocene (**Figure 9A**)

The Indian–Eurasian plate collision mainly occurred from the Early Palaeocene to Eocene, and the central Tibetan Plateau underwent weak tectonic deformation after the Oligocene. However, rollback of the subducted Indian slab occurred in the Late Oligocene along the Yarlung-Zangbo suture zone, thus leading to significant upper crustal uplift and forming a series of extensional basins along the Yarlung-Zangbo suture zone (DeCelles et al., 2011; Wang L. et al., 2013; Leary et al., 2016; Shen et al., 2019; Shen et al.,
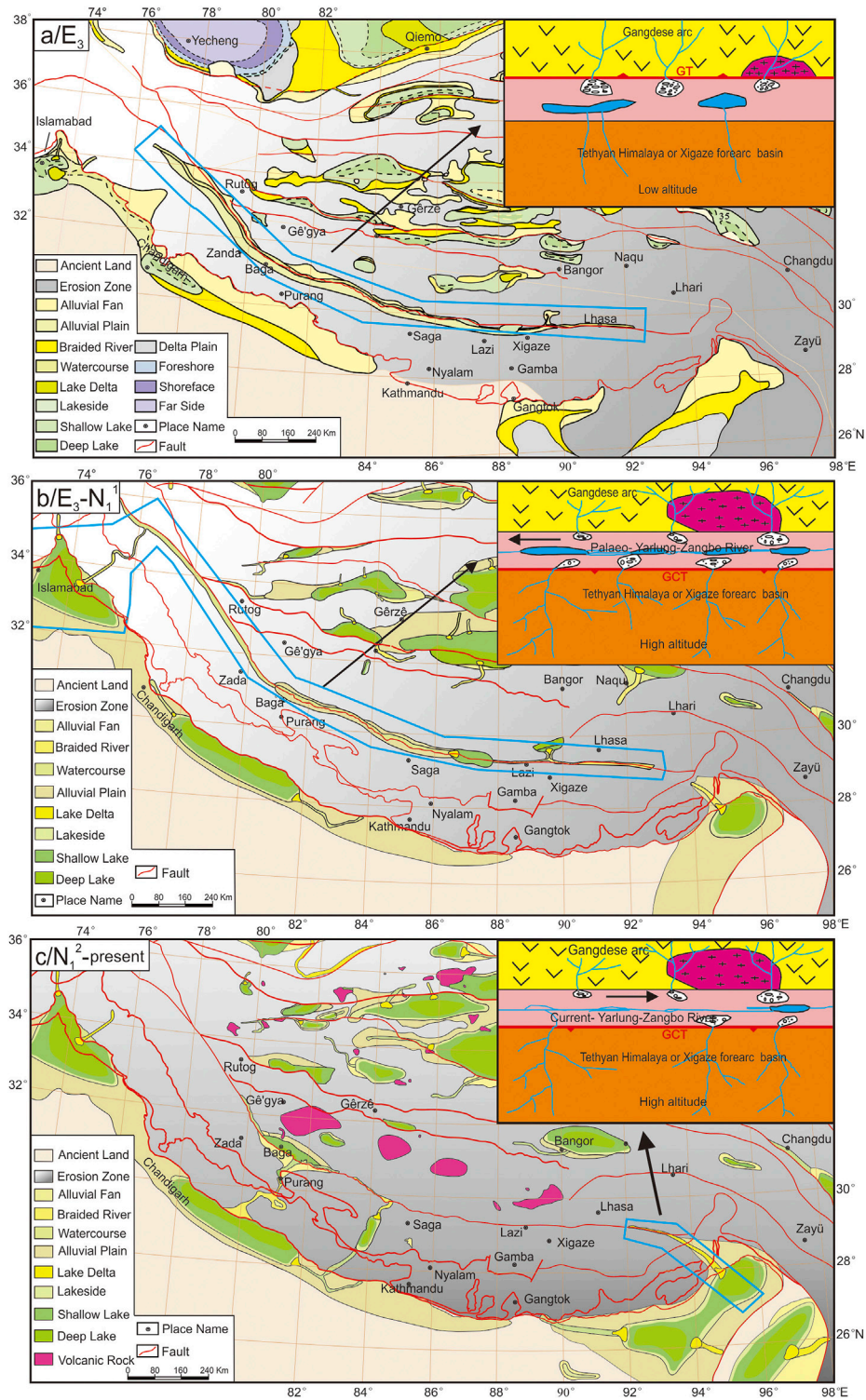
FIGURE 10 | Sketch map of evolution of palaeo-Yarlung-Zangbo River **(A,B)** and current Yarlung-Zangbo River **(C)**. (Modified after Zhang et al., 2013b)

2020). The initiation of deposition could have occurred north of the Gangdese magmatic arc and south of the Lhasa terrane above the Indian slab, subducted since ~35 Ma after the Neo-Tethyan slab breakoff at ~45 Ma (Guillot et al., 2003; Replumaz et al., 2014; Shen et al., 2019, Shen et al., 2020). The deposition of the Rigongla Formation at ~31 Ma along the northern margin of the Gangdese magmatic arc between Shiquanhe and Xigaze could correspond to this initial subsidence. Afterward, subsidence migrated southward, as the northward drifting Indian plate moved above its own stationary slab (Shen et al., 2020). Hence, around the Oligocene to Miocene, Indian slab shearing causes the southward migration of magmatism, subsidence occurred in the Gangdese magmatic arc and Indus-Yarlung suture zone, and the rocks in the south of the Gangdese and Lhasa terrane were denuded and transported to the extensional basin during this period, thus forming the thick Gangdese conglomerate. This finding is consistent with the result of our palaeocurrent and provenance studies of the Gangdese conglomerate in this period. In addition, outcrop observations of the Gangdese conglomerate on Mt. Kailas and in the Mayoumu and Xigaze areas also showed that the lower part of the Gangdese conglomerate was weakly deformed and deposited under an extensional background (**Figure 9A**).

2) Early Miocene (**Figure 9B**)

The subducted Indian plate broke off during the early Miocene, and then the Yarlung-Zangbo suture zone area changed from the previous extensional background to a compressive background (Chung et al., 2005; Replumaz et al., 2010a; Replumaz et al., 2010b; Gourbet et al., 2017). Previous studies have shown that the breakoff initiated in western Tibet and proceeded eastward (Replumaz et al., 2010a; Replumaz et al., 2010b; Capitanio et al., 2010), which is consistent with the east-to-west younging trend in adakitic magmatism between 91˚E and 95˚E (Ding and Lai, 2003; Williams et al., 2004; Liu et al., 2014) and preliminary geochronologic constraints on the age of the Gangdese conglomerate in this region. We suggest that the Gangdese conglomerate was driven by Indian slab shearing and breakoff initiated in western Tibet and proceeded eastward (Leary et al., 2016) (**Figure 9B**).

5.2 Evolution of the Palaeo-Yarlung-Zangbo River

According to the statistical analysis of the palaeocurrent direction, the palaeocurrent of the Gangdese conglomerate was generally from east to west. The lower part of the Gangdese conglomerate was mainly southward and westward; the middle to the upper part of the Gangdese conglomerate was generally westward but also showed a two-way characteristic of south and north, representing a westward axial palaeo-Yarlung-Zangbo River along the Yarlung-Zangbo suture zone during the Late Oligocene–Early Miocene. Combined with our palaeocurrent data of the Gangdese conglomerate and Cenozoic tectonic-lithofacies palaeogeographic map of Qinghai-Tibet Plateau and adjacent regions proposed by Zhang et al. (2013b), we inferred that there was a westward axial palaeo-Yarlung-Zangbo River along the whole Yarlung-Zangbo suture zone during the Late

Oligocene–Early Miocene, which presented an opposite flow to the current Yarlung-Zangbo River.

1) Southward-flowing stage (Late Oligocene, **Figure 10A**)

The development of the GT system (Late Oligocene) in southern Tibet caused the rapid uplift and denudation of the southern Gangdese arc (DeCelles et al., 2011; Wang L. et al., 2013; Leary et al., 2016; Shen et al., 2019, 2020). The Gangdese conglomerate started to accumulate in the footwall of the GT. During this time, the paleocurrents were southward, and the detritus was entirely derived from the Lhasa terrane to the north. A series of lakes might have formed along the southern margin of the Gangdese arc. An axial paleo-Yarlung-Zangbo River did not exist during this time.

2) Westward-flowing stage (Early Miocene; **Figure 10B**)

The development of the GCT system (Early Miocene) caused the uplift and denudation of the southern terranes (the Xigaze forearc basin and Tethyan Himalaya), which induced the deposition of the upper part of the Gangdese conglomerate, with increasing detritus sourced from the south. The westward-flowing palaeo-Yarlung-Zangbo River initiated during this time. As we suggest that the Gangdese conglomerate was driven by Indian slab shearing and breakoff that initiated in western Tibet and proceeded eastward (Leary et al., 2016), we inferred that the palaeo-Yarlung-Zangbo River had been headward erosion from west to east, capturing the southward flowing tributaries and lakes of the earlier stage; this is also consistent with the east youth trend age of the Gangdese conglomerate.

3) Eastward-flowing stage (Early Miocene-present; **Figure 10C**) (Zhang et al., 2013b)

Since the late middle Miocene, the palaeogeomorphology in the southern Tibetan Plateau underwent a reversal, becoming higher in the west and lower in the east. The deposition of the Gangdese conglomerate ended, and the present Yarlung-Zangbo River initiated.

6 CONCLUSION

The Oligocene–Miocene Gangdese conglomerate exposed along the Yarlung-Zangbo suture zone was deposited in an alluvial-fan and fluvial system that was dominated by conglomerate and sandstone and included minor volumes of siltstone and tuff. Based on detailed sedimentary, provenance, and chronology studies, the following conclusions can be drawn.

1) The main deposition age of the Gangdese conglomerate was likely Late Oligocene–Early Miocene, and it showed a youth trend from west to east.
2) The palaeocurrent of the Gangdese conglomerate was generally from east to west. The lower part of the

Gangdese conglomerate was mainly southward and westward; the middle to the upper part of the Gangdese conglomerate was generally westward but also showed south and north characteristics. The provenance of the Gangdese conglomerate in the lower part was mainly the Gangdese arc, Lhasa terrane, and in the upper part of the Gangdese conglomerate from the south and north side.

3) We established a sedimentary-tectonic model of the Late Oligocene–Early Miocene Gangdese conglomerate in which the Gangdese conglomerate deposited in an extensional tectonic environment in the early period and an extrusion tectonic environment in the late period, which was controlled by Indian slab shearing and breakoff during the Late Oligocene–Miocene.

4)We inferred that there was a westward axial palaeo-Yarlung-Zangbo River along the whole Yarlung-Zangbo suture zone during the Late Oligocene–Early Miocene, and its flow was opposite to that of the current Yarlung-Zangbo River.

DATA AVAILABILITY STATEMENT

The original contributions presented in the study are included in the article/**Supplementary Material**; further inquiries can be directed to the corresponding authors.

REFERENCES

Ai, K., Shi, G., Zhang, K., Ji, J., Song, B., Shen, T., et al. (2019). The Uppermost Oligocene Kailas flora from Southern Tibetan Plateau and its Implications for the Uplift History of the Southern Lhasa Terrane. *Palaeogeogr. Palaeoclimatol. Palaeoecol.* 515, 143–151. doi:10.1016/j.palaeo.2018.04.017

Aitchison, J. C., Ali, J. R., Chan, A., Davis, A. M., and Lo, C.-H. (2009). Tectonic Implications of Felsic Tuffs within the Lower Miocene Gangrinboche Conglomerates, Southern Tibet. *J. Asian Earth Sci.* 34 (3), 287–297. doi:10.1016/j.jseaes.2008.05.008

Aitchison, J. C., Ali, J. R., and Davis, A. M. (2007). When and where Did India and Asia Collide? *J. Geophys. Res.* 112 (B5), 1–19. doi:10.1029/2006JB004706

Aitchison, J. C., Davis, A. M., Badengzhu, H., and Luo, H. (2002). New Constraints on the India-Asia Collision: the Lower Miocene Gangrinboche Conglomerates, Yarlung Tsangpo Suture Zone, SE Tibet. *J. Asian Earth Sci.* 21 (3), 251–263. doi:10.1016/S1367-9120(02)00037-8

Belousova, E., Griffin, W., O'Reilly, S. Y., and Fisher, N. (2002). Igneous Zircon: Trace Element Composition as an Indicator of Source Rock Type. *Contrib. Mineral. Petrol.* 143 (5), 602–622. doi:10.1007/s00410-002-0364-7

Capitanio, F. A., Morra, G., Goes, S., Weinberg, R. F., and Moresi, L. (2010). India-asia Convergence Driven by the Subduction of the Greater Indian Continent. *Nat. Geosci* 3 (2), 136–139. doi:10.1038/ngeo725

Carrapa, B., Orme, D. A., DeCelles, P. G., Kapp, P., Cosca, M. A., and Waldrip, R. (2014). Miocene Burial and Exhumation of the India-Asia Collision Zone in Southern Tibet: Response to Slab Dynamics and Erosion. *Geology* 42 (5), 443–446. doi:10.1130/G35350.1

Chu, M.-F., Chung, S.-L., Song, B., Liu, D., O'Reilly, S. Y., Pearson, N. J., et al. (2006). Zircon U-Pb and Hf Isotope Constraints on the Mesozoic Tectonics and Crustal Evolution of Southern Tibet. *Geol* 34 (9), 745–748. doi:10.1130/G22725.1

Chung, S.-L., Chu, M.-F., Zhang, Y., Xie, Y., Lo, C.-H., Lee, T.-Y., et al. (2005). Tibetan Tectonic Evolution Inferred from Spatial and Temporal Variations in post-collisional Magmatism. *Earth-Science Rev.* 68 (3-4), 173–196. doi:10.1016/j.earscirev.2004.05.001

AUTHOR CONTRIBUTIONS

KA: Investigation, Methodology, Writing-original draft. KZ: Investigation, Supervision, Funding acquisition. BS: Investigation, Writing-review and editing. TS: Investigation, Writing-review. JJ: Investigation, Methodology.

FUNDING

ACKNOWLEDGMENTS

SUPPLEMENTARY MATERIAL

The Supplementary Material for this article can be found online at: https://www.frontiersin.org/articles/10.3389/feart.2022.808843/full#supplementary-material

DeCelles, P. G., Castañeda, I. S., Carrapa, B., Liu, J., Quade, J., Leary, R., et al. (2016). Oligocene-Miocene Great Lakes in the India-Asia Collision Zone. *Basin Res.* 30, 228–247. doi:10.1111/bre.12217

DeCelles, P. G., Gehrels, G. E., Najman, Y., Martin, A. J., Carter, A., and Garzanti, E. (2004). Detrital Geochronology and Geochemistry of Cretaceous-Early Miocene Strata of Nepal: Implications for Timing and Diachroneity of Initial Himalayan Orogenesis. *Earth Planet. Sci. Lett.* 227 (3-4), 313–330. doi:10.1016/j.epsl.2004.08.019

DeCelles, P. G., Kapp, P., Quade, J., and Gehrels, G. E. (2011). Oligocene-Miocene Kailas basin, Southwestern Tibet: Record of Postcollisional Upper-Plate Extension in the Indus-Yarlung Suture Zone. *Geol. Soc. America Bull.* 123 (7-8), 1337–1362. doi:10.1130/B30258.1

Ding, L., Kapp, P., and Wan, X. (2005). Paleocene-Eocene Record of Ophiolite Obduction and Initial India-Asia Collision, South central Tibet. *Tectonics* 24 (3), 1–18. doi:10.1029/2004TC001729

Ding, L., and Lai, Q. (2003). New Geological Evidence of Crustal Thickening in the Gangdese Block Prior to the Indo-Asian Collision. *Chin. Sci. Bull.* 48 (15), 1604–1610. doi:10.1007/BF03183969

Gansser, A. (1964). *The Geology of the Himalayas.* New York: Wiley-Interscience, 289.

Garzanti, E., Baud, A., and Mascle, G. (1987). Sedimentary Record of the Northward Flight of India and its Collision with Eurasia (Ladakh Himalaya, india). *Geodinamica Acta* 1 (4-5), 297–312. doi:10.1080/09853111.1987.11105147

Geng, G., and Tao, J. (1982). "Tertiary Plants from Xizang," in *Integrated Scientific Expedition Team to the Qinghai-Xizang Plateau, Academia Sinica the Series of the Scientific Expedition the Qinghai-Xizang Plateau. Palaeontology of Xizang (Book V)* (Beijing: Science Press), 110–123.

Gourbet, L., Mahéo, G., Leloup, P. H., Paquette, J.-L., Sorrel, P., Henriquet, M., et al. (2017). Western Tibet Relief Evolution since the Oligo-Miocene. *Gondwana Res.* 41, 425–437. doi:10.1016/j.gr.2014.12.003

Guillot, S., Garzanti, E., Baratoux, D., Marquer, D., Maheo, G., and de Sigoyer, J. (2003). Reconstructing the Total Shortening History of the NW Himalaya. *Geochemistry, Geophysics, Geosystems* 4 (7), 1064. doi:10.1029/2002GC000484

Guo, S. (1975). "The Plant of the Xigaze Group from Mount Jolmo Lungma Region," in *Tibet Scientific Expedition Team, Academia Sinica Report of Scientific Expedition to Mt. Jolmo Lungma Region* (Beijing: Science Press), 411–425.

Hu, X., Jansa, L., Chen, L., Griffin, W. L., O'Reilly, S. Y., and Wang, J. (2010). Provenance of Lower Cretaceous Wölong Volcaniclastics in the Tibetan Tethyan Himalaya: Implications for the Final Breakup of Eastern Gondwana. *Sediment. Geology.* 223 (3-4), 193–205. doi:10.1016/j.sedgeo.2009.11.008

Hu, X., Sinclair, H. D., Wang, J., Jiang, H., and Wu, F. (2012). Late Cretaceous-Palaeogene Stratigraphic and basin Evolution in the Zhepure Mountain of Southern Tibet: Implications for the Timing of India-Asia Initial Collision. *Basin Res.* 24 (5), 520–543. doi:10.1111/j.1365-2117.2012.00543.x

Ji, W. Q., Wu, F. Y., Chung, S. L., Li, J. X., and Liu, C. Z. (2009). Zircon U-Pb Geochronology and Hf Isotopic Constraints on Petrogenesis of the Gangdese Batholith, Southern Tibet. *Chem. Geology.* 262 (3-4), 229–245. doi:10.1016/j.chemgeo.2009.01.020

Kapp, P., DeCelles, P. G., Gehrels, G. E., Heizler, M., and Ding, L. (2007). Geological Records of the Lhasa-Qiangtang and Indo-Asian Collisions in the Nima Area of central Tibet. *Geol. Soc. America Bull.* 119 (7-8), 917–933. doi:10.1130/B26033.1

Kexin, Z., Guocan, W., Yadong, X., Mansheng, L., Junliang, J., Guoqiao, X., et al. (2013a). Sedimentary Evolution of the Qinghai-Tibet Plateau in Cenozoic and its Response to the Uplift of the Plateau. *Acta Geologica Sinica-English Edition* 87 (2), 555–575. doi:10.1111/1755-6724.12068

Kong, M., Jiang, W., and Liu, C. (2015). LA-ICP-MS Zircon U-Pb Age of Interbedded Volcanic Rocks in the Lobuza Group, Tibet and its Significance. *Geol. Bull. China* 34 (Z1), 328–336. doi:10.3969/j.issn.1671-2552.2015.02.010

Leary, R., Orme, D. A., Laskowski, A. K., DeCelles, P. G., Kapp, P., Carrapa, B., et al. (2016). Along-strike Diachroneity in Deposition of the Kailas Formation in central Southern Tibet: Implications for Indian Slab Dynamics. *Geosphere* 12 (4), 1198–1223. doi:10.1130/GES01325.1

Li, J.-g., Guo, Z.-y., Batten, D. J., Cai, H.-w., and Zhang, Y.-y. (2010). Palynological Stratigraphy of the Late Cretaceous and Cenozoic Collision-Related Conglomerates at Qiabulin, Xigaze, Xizang (Tibet) and its Bearing on Palaeoenvironmental Development. *J. Asian Earth Sci.* 38 (3-4), 86–95. doi:10.1016/j.jseaes.2009.10.001

Li, J. (2004). Discovery and Preliminary Study on Palynofossils from the Cenozoic Qiuwu Formation of Xizang (Tibet). *Acta Micropalaeontologica Sinica* 21, 216–221. doi:10.3969/j.issn.1000-0674.2004.02.010

Li, J., Guo, Z., and Zhang, Y. (2009). Palynofloral Assemblages from the Dagzhuka Formation at Qiabulin, Xigaze, Xizang (Tibet): Their Age and Bearing on Palaeoenvironments and Palaeogeography. *Acta Palaeontologica Sinica* 48, 163–174. doi:10.3969/j.issn.0001-6616.2009.02.005

Li, S., Ding, L., Xu, Q., Wang, H., Yue, Y., and Baral, U. (2017). The Evolution of Yarlung Tsangpo River: Constraints from the Age and Provenance of the Gangdese Conglomerates, Southern Tibet. *Gondwana Res.* 41, 249–266. doi:10.1016/j.gr.2015.05.010

Liu, D., Zhao, Z., Zhu, D.-C., Niu, Y., DePaolo, D. J., Harrison, T. M., et al. (2014). Postcollisional Potassic and Ultrapotassic Rocks in Southern Tibet: Mantle and Crustal Origins in Response to India-Asia Collision and Convergence. *Geochimica et Cosmochimica Acta* 143, 207–231. doi:10.1016/j.gca.2014.03.031

Miall, A. D. (1984). *Principles of Sedimentary basin Analysis*. New York: Springer-Verlag, 668.

Miall, A. D. (1996). *The Geology of Fluvial Deposits: Sedimentary Facies, Basin Analysis and Petroleum Geology*. Berlín: Springer-Verlag.

Replumaz, A., Capitanio, F. A., Guillot, S., Negredo, A. M., and Villaseñor, A. (2014). The Coupling of Indian Subduction and Asian continental Tectonics. *Gondwana Res.* 26 (2), 608–626. doi:10.1016/j.gr.2014.04.003

Replumaz, A., Negredo, A. M., Guillot, S., and Villaseñor, A. (2010a). Multiple Episodes of continental Subduction during India/Asia Convergence: Insight from Seismic Tomography and Tectonic Reconstruction. *Tectonophysics* 483 (1-2), 125–134. doi:10.1016/j.tecto.2009.10.007

Replumaz, A., Negredo, A. M., Villaseñor, A., and Guillot, S. (2010b). Indian continental Subduction and Slab Break-Off during Tertiary Collision. *Terra Nova* 22 (4), 290–296. doi:10.1111/j.1365-3121.2010.00945.x

Shen, T., Wang, G., Bernet, M., Replumaz, A., Ai, K., Song, B., et al. (2019). Long-term Exhumation History of the Gangdese Magmatic Arc: Implications for the Evolution of the Kailas Basin, Western Tibet. *Geol. J.* 55 (11), 7239–7250. doi:10.1002/gj.3539

Shen, T., Wang, G., Replumaz, A., Husson, L., Webb, A. A. G., Bernet, M., et al. (2020). Miocene Subsidence and Surface Uplift of Southernmost Tibet Induced by Indian Subduction Dynamics. *Geochem. Geophys. Geosyst.* 21 (10), e2020GC009078. doi:10.1029/2020GC009078

Wang, J.-G., Hu, X.-M., Garzanti, E., and Wu, F.-Y. (2013a). Upper Oligocene-Lower Miocene Gangrinboche Conglomerate in the Xigaze Area, Southern Tibet: Implications for Himalayan Uplift and Paleo-Yarlung-Zangbo Initiation. *J. Geology.* 121 (4), 425–444. doi:10.1086/670722

Wang, J., Hu, X., Jansa, L., and Huang, Z. (2011). Provenance of the Upper Cretaceous-Eocene Deep-Water Sandstones in Sangdanlin, Southern Tibet: Constraints on the Timing of Initial India-Asia Collision. *J. Geology.* 119 (3), 293–309. doi:10.1086/659145

Wang, L., Pan, G., and Ding, J. (2013b). *1:1 500000 Geological Map of Qinghai-Tibet Plateau and Adjacent Areas*. Chengdu, China: Chengdu Cartographic Publishing House.

Wen, D., Liu, D., Chung, S., Chu, M., Ji, J., Zhang, Q., et al. (2008). Zircon SHRIMP U-Pb Ages of the Gangdese Batholith and Implications for Neotethyan Subduction in Southern Tibet. *Chem. Geology.* 252 (3-4), 191–201. doi:10.1016/j.chemgeo.2008.03.003

Williams, H. M., Turner, S. P., Pearce, J. A., Kelley, S. P., and Harris, N. B. W. (2004). Nature of the Source Regions for post-collisional, Potassic Magmatism in Southern and Northern Tibet from Geochemical Variations and Inverse Trace Element Modelling. *J. Petrol.* 45 (3), 555–607. doi:10.1093/petrology/egg094

Yin, A. (2006). Cenozoic Tectonic Evolution of the Himalayan Orogen as Constrained by Along-Strike Variation of Structural Geometry, Exhumation History, and Foreland Sedimentation. *Earth-Science Rev.* 76, 1–131. doi:10.1016/j.earscirev.2005.05.004

Yin, A., Harrison, T. M., Murphy, M. A., Grove, M., Nie, S., Ryerson, F. J., et al. (1999). Tertiary Deformation History of southeastern and Southwestern Tibet during the Indo-Asian Collision. *Geol. Soc. America Bull.* 111, 1644–1664. doi:10.1130/0016-7606(1999)111<1644:tdhosa>2.3.co;2

Yin, A., Harrison, T. M., Ryerson, F. J., Wenji, C., Kidd, W. S. F., and Copeland, P. (1994). Tertiary Structural Evolution of the Gangdese Thrust System, southeastern Tibet. *J. Geophys. Res.* 99 (B9), 18175–18201. doi:10.1029/94JB00504

Zhang, K., Wang, G., Luo, M., Xu, Y., and Song, B. (2013b). *Cenozoic Tectonic-Lithofacies Palaeogeographic Map and Manual of Qinghai-Tibet Plateau and Adjacent Regions (1:3000000)*. Beijing, China: Beijing Geological publishing house, 1–299.

Zhu, D.-C., Zhao, Z.-D., Niu, Y., Mo, X.-X., Chung, S.-L., Hou, Z.-Q., et al. (2011). The Lhasa Terrane: Record of a Microcontinent and its Histories of Drift and Growth. *Earth Planet. Sci. Lett.* 301 (1-2), 241–255. doi:10.1016/j.epsl.2010.11.005